

Lithium-Ion Dynamics in an All-Solid-State Lithium Battery Observed by In-Situ Electron Holography

Kazuo Yamamoto,^{1*} Yasutoshi Iriyama,^{2*} Toru Asaka,¹ Tsukasa Hirayama,¹ Hideki Fujita,¹ Katsumasa Nonaka,³ Koji Miyahara,³ Yuji Sugita,³ and Zempachi Ogumi⁴

¹ Nanostructures Research Laboratory, Japan Fine Ceramics Center, Japan.

² Department of Materials Science and Chemical Engineering, Shizuoka University, Japan.

³ Chubu Electric Power Co., Inc., Japan.

⁴ Innovative Collaboration Center, Kyoto University, Japan.

All-solid-state lithium batteries (LIBs) having incombustible solid-electrolytes have been expected to be candidates of next generation batteries because they can solve safety problems, prevent liquid-electrolyte spills, and reduce the needless side reactions at the electrode/electrolyte interface. However, only small thin-film LIBs have so far been put into practical use in low-power consumption devices. This is mainly due to the large resistance of Li^+ transfer at the electrode/solid-electrolyte interface. Despite extensive efforts to analyze reaction mechanisms at the interface, it has not been possible to visualize the electric potential across working batteries. Dynamic observation of the potential across the interface would help identify sources of resistance, enabling more efficient and robust batteries to be developed through a combination of nano-engineering and materials design. With this objective, we used in-situ electron holography (EH) to directly observe the potential change resulting from Li-ion diffusion in micron-scale LIBs operated within a TEM [1,2].

Figure 1(a) illustrates the prepared battery sample. A $90\ \mu\text{m}\ \text{Li}_{1+x+y}\text{Al}_y\text{Ti}_{2-y}\text{Si}_x\text{P}_{3-x}\text{O}_{12}$ (LATSP0)[3] sheet was used as the solid electrolyte. An 800 nm of a LiCoO_2 positive electrode was deposited on one side of the sheet by PLD. Then, the Au and Pt films were deposited as current collectors. A negative electrode was formed in-situ during EH observation around the LATSP0/Pt interface by decomposing the LATSP0 with excess Li insertion reaction [4]. To observe how the Li^+ s move and form the negative electrode material, both electrode/solid-electrolyte interface regions within the red boxes in Fig. 1(a) were thinned by a 40-kV FIB to a thickness of about 60 nm. The sample was loaded on a TEM holder that had two fixed electrodes for applying voltage to the sample. Figures 1(b) and 1(c) show TEM images around both interfaces in the pristine state (0 V), respectively. Figure 1(d) plots the initial cyclic voltammogram (CV) with a potential sweep rate of $40\ \text{mV}\ \text{min}^{-1}$. A pair of redox peaks is observed around 1.6 V, which means that the sample works as a LIB.

During the initial CV measurement, holograms around both interfaces were taken at a given voltage indicated by arrows in Fig. 1(d). The electric potential profiles along the positive side "A"- "B" and the negative side "C"- "D", surrounded by dotted lines in Figs. 1(b) and 1(c), were reconstructed from the holograms. To remove the background phase due to variation of inner potential of the sample and charging by incident electrons, the initial state measured at zero bias was subtracted from each reconstructed phase image.

Figures 2(a)–2(f) are the profiles near the LiCoO_2 /LATSP0 interface, and Figs. 2(g)–2(l) are those near the LATSP0/Pt interface. The lowercase letters in the figures correspond to those in the CV plot (Fig. 1(d)). The potential in the vertical axis is the relative value against the flat potential level (we set it as 0 V) so as to see how much potential is distributed around the positive and negative side interfaces. The significant potential was formed within $3\ \mu\text{m}$ regions around the interfaces. At 0.42 V (Fig. 2(g)), no potential was distributed in the negative side, so the voltage was mainly applied to the positive side. Figure 2(a) shows the positive-side potential distribution at 0.72 V. The linear slope in the LiCoO_2 electrode resulted from a shift of the electrical band structures caused by extracting Li^+ s, which indicates a subtle difference in the Li^+ concentration in the electrode. Also, note that the steep

potential drop was presented at the positive-side interface. The gradual potential slope in the LATSPo sheet indicated by the dashed red curve was possibly due to the Li^+ -poor region from which some Li^+ s moved away. At 1.05 V (Figs. 2(b) and 2(h)), the negative-side potential-change also appeared within 3 μm in distance from the interface, and the potential slope changed at a significant point (red arrow position), about 700 nm from the interface. This negatively charged region was the in-situ formed negative electrode material fabricated during the initial charging process. When the voltage was increased to 1.53 V (Figs. 2(c) and 2(i)) and 1.95 V (Figs. 2(d) and 2(j)), the positive-side potential was almost totally maintained. However, the negative-side one was distributed more deeply, especially at the right side of the red arrow. When the voltage was swept down to 1.48 V (Figs. 2(e) and 2(k)) and 1.26 V (Figs. 2(f) and 2(l)) at the discharged state, a different potential distribution was formed on both sides. On the positive side, a flat potential distribution was newly observed inside the LATSPo sheet around the interface. The flat range was 300 nm at 1.48 V, which decreased to 210 nm at 1.26 V. This was probably due to the Li^+ s accumulated around the interface because of the high interfacial resistance ($4000 \Omega \text{ cm}^2$). On the negative side, the gentle slope on the left side of the red arrow almost flattened out compared with those of Figs. 2(h)–2(j) in the charged state. Instead, a slightly lower potential ($\sim 0.08 \text{ V}$) appeared in a region about 1600 nm wide, moving this region 300 nm to the left between 1.48 V and 1.26 V. Because this region had no significant TEM contrast, a small amount of Li^+ s might be trapped, which retarded the Li^+ movement in the LATSPo solid electrolyte.

In summary, we have carried out a charge-discharge reaction of an all-solid-state Li battery in a TEM and visualized the entire potential distribution change during the reaction by EH. EH clearly detected a unique formation process of negative electrode material from the parent solid electrolyte. Moreover, the retardant regions of the Li^+ transfer in the battery were detected. The in-situ electrochemical electron holography method is a cutting-edge technology with which to clarify where the resistive region is presented in a battery.

References

- [1] K. Yamamoto et al., *Angew. Chem. Int. Ed.* **49** (2010) 4414.
- [2] K. Yamamoto et al., *Electrochem. Comm.* (submitted).
- [3] J. Fu, *J. Am. Ceram. Soc.* **80** (1997) 1901.
- [4] Y. Iriyama et al., *Electrochem. Comm.* **8** (2006) 1287.

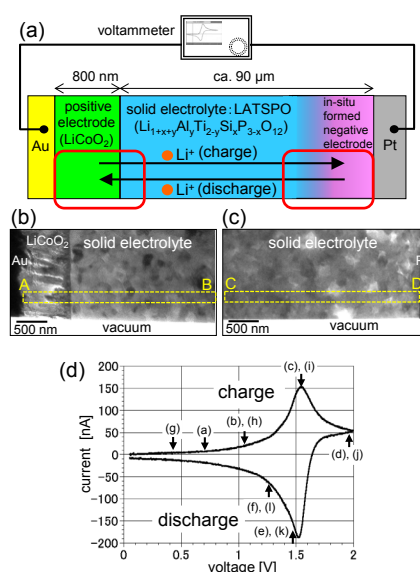


Figure 1 Prepared battery sample, (a) illustration of the battery sample, (b), (c) TEM images around the interfaces, (d) cyclic voltammogram measured in a TEM

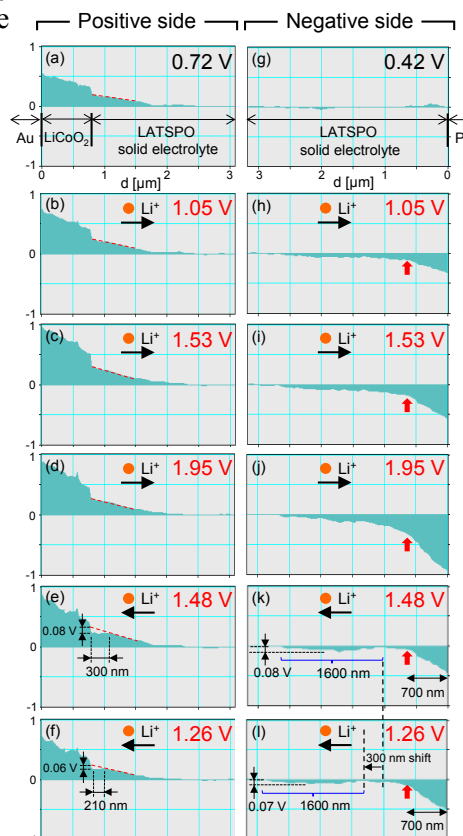


Figure 2 Electric potential profiles obtained from the line "A"- "B" and "C"- "D" indicated in Figs. 1(b) and 1(c), (a) - (f) profiles around the positive side, (g) - (l) profiles around the negative side.